

# CONFORMAL FDTD MODELING OF 3-D WAKE FIELDS

T. G. Jurgens and F. A. Harfoush  
*Fermi National Accelerator Laboratory\**  
*Batavia, Illinois 60510*

## Abstract

Many computer codes have been written to model wake fields. Here we describe the use of the Conformal Finite Difference Time Domain (CFDTD) method to model the wake fields generated by a rigid beam traveling through various accelerating structures. The non-cylindrical symmetry of some of the problems considered here requires the use of a three dimensional code. In traditional FDTD codes, curved surfaces are approximated by rectangular steps. The errors introduced in wake field calculations by such an approximation can be reduced by increasing the mesh size, therefore increasing the cost of computing. Another approach, validated here, deforms Ampere and Faraday contours near a media interface so as to conform to the interface. These improvements to the FDTD method result in better accuracy of the fields at asymptotically no computational cost. This method is also capable of modeling thin wires as found in beam profile monitors, and slots and cracks as found in resistive wall monitors.

## I. INTRODUCTION

This paper discusses the full three dimensional contour FDTD modeling of accelerator wake fields. Previously, the present authors reported [1] on a two dimensional Ampere and Faraday laws based CFDTD computer code for particle accelerator modeling. That paper also summarized other areas to which CFDTD has been applied. These applications include the modeling of slots, cracks and wires which have subcell dimensions. More recently, other investigators [2] have written about their investigations of two dimensional Ampere-Faraday laws based FDTD algorithms.

## II. THE CONTOUR FDTD METHODOLOGY

Rather than starting with Maxwell's curl equations, the discussion of the contour FDTD method begins with Ampere's and Faraday's laws, shown here for reference.

$$\oint_C \vec{H} \cdot d\vec{l} = \iint_S \sigma \vec{E} \cdot d\vec{S} + \frac{\partial}{\partial t} \iint_S \vec{D} \cdot d\vec{S} + \iint_S \rho \vec{v} \cdot d\vec{S} \quad (1)$$

$$\oint_C \vec{E} \cdot d\vec{l} = -\frac{\partial}{\partial t} \iint_S \vec{B} \cdot d\vec{S} \quad (2)$$

These equations describe two intersecting contour integrals with enclosed surface integrals as illustrated in Figure 1.

\*Operated by the Universities Research Association under contract with the U.S. Department of Energy

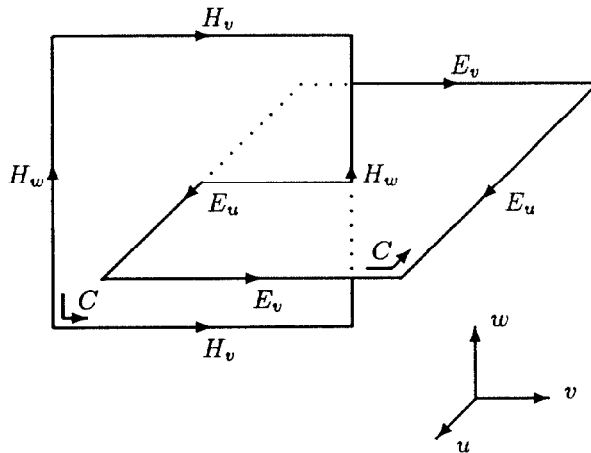


Figure 1: Intersecting Ampere and Faraday Contours

The electric and magnetic fields are temporally updated in a leap-frog manner. The  $\rho \vec{v}$  term in equation 1 accounts for the movement of charge in the contour FDTD grid.

When the contour paths are rectangular, discretization of the integrals result in difference equations that are identical to those found in the traditional curl-equation based FDTD method. In the contour FDTD implementation only the contours near media interfaces are deformed. This permits the accurate modeling curved surfaces. Since the number of distorted contours scales as the surface area of an object, while the problem space scales as its volume, the additional computing cost incurred by including these contours is negligible.

As an illustration of the CFDTD technique, a distorted Faraday contour near a perfect conductor will be studied. In this example the contour is deformed as indicated in Figure 2. The contour segments are numbered from one to four, counterclockwise from the bottom. The fields are assumed constant along each segment, including the segment along the media interface. The temporal derivatives are replaced with a second order accurate central difference approximation. The discretization of Faraday's law for this contour is:

$$H_x^{n+\frac{1}{2}}(i, j+1/2, k+1/2) = H_x^{n-\frac{1}{2}}(i, j+1/2, k+1/2) + \frac{\Delta t}{A\mu(i, j+1/2, k+1/2)} [l_3 E_y^n(i, j+1/2, k+1) - \quad (3)$$

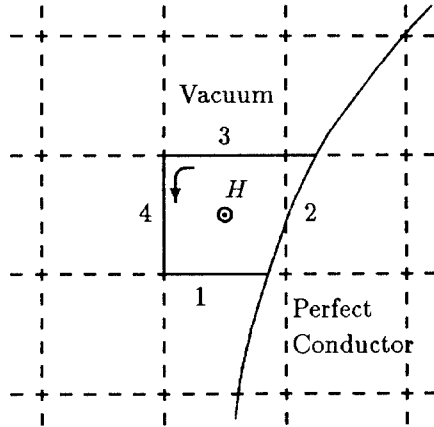


Figure 2: A Distorted Faraday Contour

$$l_1 E_y^n(i, j + 1/2, k) + l_4 E_z^n(i, j, k + 1/2) - l_2 E_t^n(\text{on surface})]$$

where  $A$  is the area the contour encircles,  $l_p$  is the length of the  $p^{\text{th}}$  segment of the contour,  $E_t$  is the component of the electric field tangential to the surface,  $\Delta t$  is the temporal increment, and  $i, j, k$  and  $n$  are the indices of the discretization. The last term in this equation is equal to zero since this electric field component is tangent to the perfectly conducting surface.

### III. SIMULATION RESULTS

#### A. Empty Beam Pipe

In order to validate the numerical model, the contour FDTD predicted fields were compared to analytical results for a simple geometry. The electric field produced by a line charge with velocity  $v = c$  traveling along the axis of a circular beam pipe is given by [3]:

$$|\vec{E}| = \frac{\lambda}{2\pi\epsilon_0} \frac{1}{r} \delta(z - ct) \quad (4)$$

where  $\lambda$  is the linear charge density in coulombs per meter and  $r$  is the radial distance from the line charge in meters. The numerical simulation employed a fairly coarse gridding of eleven cells for the radius, with the contours adjacent to the beam pipe distorted to conform to the pipe's curvature. The cell size was 0.006 meters. A two dimensional cut, which is perpendicular to the pipe axis, of the contour geometry is pictured in Figure 3. The walls of the pipe were modeled as perfectly conducting. A comparison of the contour FDTD computed results and the analytical results, graphed in Figure 4, are in good agreement, typically within 3%.

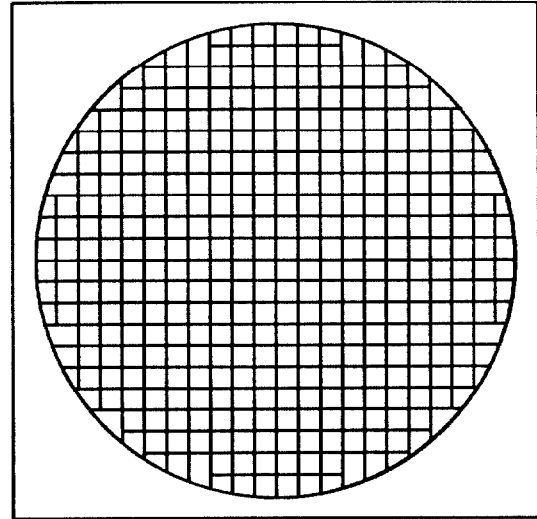


Figure 3: A 2D Cut, Perpendicular to the Pipe Axis, of the CFDTD Contours

#### Comparison of Analytical and FDTD Results in an Empty Beam Pipe

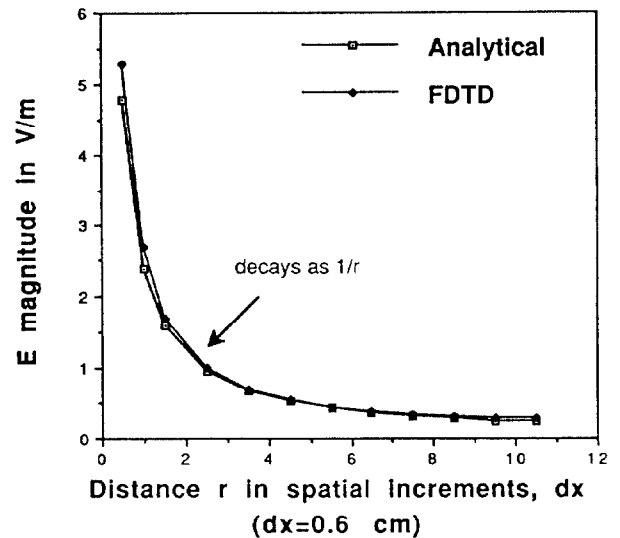


Figure 4: The Electric Field Magnitude of a Line Charge, velocity =  $c$ , Contour FDTD vs Analytical Expression

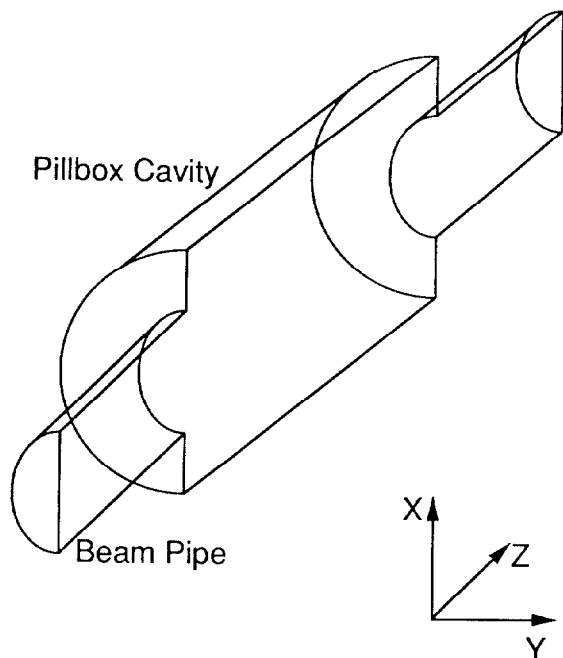


Figure 5: Beam Pipe with a Pillbox

#### B. Pillbox in a Beam Pipe

The next geometry modeled was a beam pipe containing a circular pillbox, illustrated in Figure 5. The beam pipe radius was 6.6 cm and the pillbox radius 19.8 cm. As before, the cell size was 0.6 cm. The beam was a moving line charge, with velocity =  $c$  and a gaussian axial charge distribution.

Simulations for an axially located beam as well as an off axis beam were computed. The passage of the beam through the pillbox excited various modes in the pillbox. A study of the time history of the pillbox fields for on axis excitation revealed that the  $TM_{010}$  mode primarily was excited. A video movie including these two simulations was produced [4].

#### C. Pillbox in a Beam Pipe with Flat Plates

The next geometry modeled was a beam pipe containing a circular pillbox with flat plates located in the pillbox and, further downstream, in the beam pipe. Note that this geometry requires the use of a full three dimensional code. Once again, both on axis beam and an off axis beam excitations were modeled. The on axis beam excited a  $TM_{010}$  mode in the pillbox with flat plates. The resonance of the downstream beam pipe and flat plate structure was weak and difficult to characterize. The aforementioned movie [4] contains these simulations as well.

### IV. CONCLUSION

This paper validated the CFDTD algorithm for full three dimensional modeling of wake fields. The CFDTD methodology was explained and various simulations were

summarized. Future enhancements to the CFDTD accelerator code include the ability to model frequency dispersive media and the self consistent incorporation of charge movement.

### V. REFERENCES

- [1] T. G. Jurgens and F. A. Harfoush, "Finite Difference Time Domain Modelling of Particle Accelerators," *IEEE 1989 Particle Accelerator Conference*, Chicago, Illinois, March 1989.
- [2] C. C. Shang and J. F. DeFord, "Modified Yee Field Solutions in the AMOS Wakefield Code," *Proceedings of the 1990 Linear Accelerator Conference*, Albuquerque, New Mexico, September 1990.
- [3] A. W. Chao, SLAC-PUB-2946, June 1982.
- [4] F. A. Harfoush and T. G. Jurgens, "Visualization of Wake Fields in 3-D," *IEEE 1991 Particle Accelerator Conference*, San Francisco, California, QGR-10, May 1991.